

Analysis and Evaluation of Pumping Test Data

Second Edition (Completely Revised)

Analysis and Evaluation of Pumping Test Data

Second Edition (Completely Revised)

G.P. Kruseman

Senior hydrogeologist, TNO Institute of Applied Geoscience, Delft

N.A. de Ridder

Senior hydrogeologist, International Institute for Land Reclamation
and Improvement, Wageningen

and

Professor in Hydrogeology, Free University, Amsterdam

With assistance from

J.M. Verweij

Freelance hydrogeologist

Publication 47



International Institute for Land Reclamation and Improvement,
P.O. Box 45, 6700 AA Wageningen, The Netherlands, 1994.

The first edition of this book appeared as No. 11 in the series of Bulletins of the International Institute for Land Reclamation and Improvement/ILRI. Because the ILRI Bulletins have now been discontinued, this completely revised edition of the book appears as ILRI Publication 47.

The production of the book was made possible by cooperation between the following institutions:

International Institute for Land Reclamation and Improvement, Wageningen
TNO Institute of Applied Geoscience, Delft

Institute for Earth Sciences, Free University/VU, Amsterdam

First Edition 1970

Reprinted 1973

Reprinted 1976

Reprinted 1979

Reprinted 1983

Reprinted 1986

Reprinted 1989

Second Edition

Reprinted 1991

Reprinted 1992

Reprinted 1994

Reprinted 2000

The aims of ILRI are:

- To collect information on land reclamation and improvement from all over the world;
- To disseminate this knowledge through publications, courses, and consultancies;
- To contribute - by supplementary research - towards a better understanding of the land and water problems in developing countries.

© 2000 International Institute for Land Reclamation and Improvement/ILRI. All rights reserved. This book or any part thereof may not be reproduced in any form without written permission of the publisher. Printed in The Netherlands by Veenman drukkers, Ede

ISBN 90 70754 207

Contents

Preface

1	Basic concepts and definitions	13
1.1	Aquifer, aquitard, and aquiclude	13
1.2	Aquifer types	14
1.2.1	Confined aquifer	14
1.2.2	Unconfined aquifer	14
1.2.3	Leaky aquifer	14
1.3	Anisotropy and heterogeneity	14
1.4	Bounded aquifers	17
1.5	Steady and unsteady flow	17
1.6	Darcy's law	18
1.7	Physical properties	19
1.7.1	Porosity (n)	19
1.7.2	Hydraulic conductivity (K)	21
1.7.3	Interporosity flow coefficient (λ)	21
1.7.4	Compressibility (α and β)	22
1.7.5	Transmissivity (KD or T)	22
1.7.6	Specific storage (S_s)	22
1.7.7	Storativity (S)	23
1.7.8	Storativity ratio (ω)	23
1.7.9	Specific yield (S_y)	23
1.7.10	Diffusivity (KD/S)	24
1.7.11	Hydraulic resistance (c)	24
1.7.12	Leakage factor (L)	25
2	Pumping tests	27
2.1	The principle	27
2.2	Preliminary studies	27
2.3	Selecting the site for the well	28
2.4	The well	28
2.4.1	Well diameter	28
2.4.2	Well depth	29
2.4.3	Well screen	29
2.4.4	Gravel pack	30
2.4.5	The pump	30
2.4.6	Discharging the pumped water	31
2.5	Piezometers	31
2.5.1	The number of piezometers	32

2.5.2	Their distance from the well	33
2.5.3	Depth of the piezometers	37
2.6	The measurements to be taken	37
2.6.1	Water-level measurements	38
2.6.1.1	Water-level-measuring devices	40
2.6.2	Discharge-rate measurements	41
2.6.2.1	Discharge-measuring devices	42
2.7	Duration of the pumping test	43
2.8	Processing the data	44
2.8.1	Conversion of the data	44
2.8.2	Correction of the data	44
2.8.2.1	Unidirectional variation	45
2.8.2.2	Rhythmic fluctuations	45
2.8.2.3	Non-rhythmic regular fluctuations	46
2.8.2.4	Unique fluctuations	47
2.9	Interpretation of the data	48
2.9.1	Aquifer categories	48
2.9.2	Specific boundary conditions	51
2.10	Reporting and filing of data	53
2.10.1	Reporting	53
2.10.2	Filing of data	53
3	Confined aquifers	55
3.1	Steady-state flow	56
3.1.1	Thiem's method	56
3.2	Unsteady-state flow	61
3.2.1	Theis's method	61
3.2.2	Jacob's method	65
3.3	Summary	70
4	Leaky aquifers	73
4.1	Steady-state flow	76
4.1.1	De Glee's method	76
4.1.2	Hantush-Jacob's method	77
4.2	Unsteady-state flow	80
4.2.1	Walton's method	81
4.2.2	Hantush's inflection-point method	85
4.2.3	Hantush's curve-fitting method	90
4.2.4	Neuman-Witherspoon's method	93
4.3	Summary	97

5	Unconfined aquifers	99
5.1	Unsteady-state flow	102
5.1.1	Neuman's curve-fitting method	102
5.2	Steady-state flow	106
5.2.1	Thiem-Dupuit's method	107
6	Bounded aquifers	109
6.1	Bounded confined or unconfined aquifers, steady-state flow	110
6.1.1	Dietz's method, one or more recharge boundaries	110
6.2	Bounded confined or unconfined aquifers, unsteady-state flow	112
6.2.1	Stallman's method, one or more boundaries	112
6.2.2	Hantush's method (one recharge boundary)	117
6.3	Bounded leaky or confined aquifers, unsteady-state flow	120
6.3.1	Vandenberg's method (strip aquifer)	120
7	Wedge-shaped and sloping aquifers	125
7.1	Wedge-shaped confined aquifers, unsteady-state flow	125
7.1.1	Hantush's method	125
7.2	Sloping unconfined aquifers, steady-state flow	127
7.2.1	Culmination-point method	127
7.3	Sloping unconfined aquifers, unsteady-state flow	128
7.3.1	Hantush's method	128
8	Anisotropic aquifers	133
8.1	Confined aquifers, anisotropic on the horizontal plane	133
8.1.1	Hantush's method	133
8.1.2	Hantush-Thomas's method	139
8.1.3	Neuman's extension of the Papadopulos method	140
8.2	Leaky aquifers, anisotropic on the horizontal plane	144
8.2.1	Hantush's method	144
8.3	Confined aquifers, anisotropic on the vertical plane	145
8.3.1	Week's method	145
8.4	Leaky aquifers, anisotropic on the vertical plane	147
8.4.1	Week's method	147
8.5	Unconfined aquifers, anisotropic on the vertical plane	148

9	Multi-layered aquifer systems	151
9.1	Confined two-layered aquifer systems with unrestricted cross flow, unsteady-state flow	152
9.1.1	Javandel-Witherspoon's method	152
9.2	Leaky two-layered aquifer systems with crossflow through aquitards, steady-state flow	154
9.2.1	Bruggeman's method	155
10	Partially penetrating wells	159
10.1	Confined aquifers, steady-state flow	159
10.1.1	Huisman's correction method I	162
10.1.2	Huisman's correction method II	162
10.2	Confined aquifers, unsteady-state flow	162
10.2.1	Hantush's modification of the Theis method	162
10.2.2	Hantush's modification of the Jacob method	167
10.3	Leaky aquifers, steady-state flow	169
10.4	Leaky aquifers, unsteady-state flow	169
10.4.1	Weeks's modifications of the Walton and the Hantush curve-fitting methods	169
10.5	Unconfined anisotropic aquifers, unsteady-state flow	170
10.5.1	Streltsova's curve-fitting method	170
10.5.2	Neuman's curve-fitting method	172
11	Large-diameter wells	175
11.1	Confined aquifers, unsteady-state flow	175
11.1.1	Papadopoulos's curve-fitting method	175
11.2	Unconfined aquifers, unsteady-state flow	177
11.2.1	Boulton-Streltsova's curve-fitting method	177
12	Variable-discharge tests and tests in well fields	181
12.1	Variable discharge	181
12.1.1	Confined Aquifers, Birsoy-Summer's method	181
12.1.2	Confined aquifers, Aron-Scott's method	185
12.2	Free-flowing wells	187
12.2.1	Confined aquifers, unsteady-state flow, Hantush's method	188
12.2.2	Leaky aquifers, steady-state flow, Hantush-De Glee's method	189
12.3	Well field	189
12.3.1	Cooper-Jacob's method	189

13	Recovery tests	193
13.1	Recovery tests after constant-discharge tests	194
13.1.1	Confined aquifers, Theis's recovery method	194
13.1.2	Leaky aquifers, Theis's recovery method	195
13.1.3	Unconfined aquifers, Theis's recovery method	196
13.1.4	Partially penetrating wells, Theis's recovery method	196
13.2	Recovery tests after constant-drawdown tests	196
13.3	Recovery tests after variable-discharge tests	196
13.3.1	Confined aquifers, Birsoy-Summers's recovery method	196
14	Well-performance tests	199
14.1	Step-drawdown tests	200
14.1.1	Hantush-Bierschenk's method	201
14.1.2	Eden-Hazel's method (confined aquifers)	205
14.1.3	Rorabaugh's method	209
14.1.4	Sheahan's method	212
14.2	Recovery tests	215
14.2.1	Determination of the skin factor	215
15	Single-well tests with constant or variable discharges and recovery tests	219
15.1	Constant-discharge tests	220
15.1.1	Confined aquifers, Papadopulos-Cooper's method	220
15.1.2	Confined aquifers, Rushton-Singh's ratio method	221
15.1.3	Confined and leaky aquifers, Jacob's straight-line method	223
15.1.4	Confined and leaky aquifers, Hurr-Worthington's method	226
15.2	Variable-discharge tests	229
15.2.1	Confined aquifers, Birsoy-Summers's method	229
15.2.2	Confined aquifers, Jacob-Lohman's free-flowing-well method	230
15.2.3	Leaky aquifers, Hantush's free-flowing-well method	231
15.3	Recovery tests	232
15.3.1	Theis's recovery method	232
15.3.2	Birsoy-Summers's recovery method	233
15.3.3	Eden-Hazel's recovery method	233

16	Slug tests	237
16.1	Confined aquifers, unsteady-state flow	238
16.1.1	Cooper's method	238
16.1.2	Uffink's method for oscillation tests	241
16.2	Unconfined aquifers, steady-state flow	244
16.2.1	Bouwer-Rice's method	244
17	Uniformly-fractured aquifers, double-porosity concept	249
17.1	Introduction	249
17.2	Bourdet-Gringarten's curve-fitting method (observation wells)	251
17.3	Kazemi's et al.'s straight-line method (observation wells)	254
17.4	Warren-Root's straight-line method (pumped well)	257
18	Single vertical fractures	263
18.1	Introduction	263
18.2	Gringarten-Witherspoon's curve-fitting method for observation wells	265
18.3	Gringarten et al.'s curve-fitting method for the pumped well	269
18.4	Ramey-Gringarten's curve-fitting method	271
19	Single vertical dikes	275
19.1	Introduction	275
19.2	Curve-fitting methods for observation wells	277
19.2.1	Boonstra-Boehmer's curve fitting method	277
19.2.2	Boehmer-Boonstra's curve-fitting method	279
19.3	Curve-fitting methods for the pumped well	280
19.3.1	For early and medium pumping times	280
19.3.2	For late pumping times	282
	Annexes	289
	References	367
	Author's index	373

it is horizontal, parallel, and perpendicular to the fracture. This flow regime gradually changes, until, at late time, it becomes pseudo-radial. The shapes of the curves at late time resemble those of Parts A and A' of Figure 2.12. (We return to this subject in Section 18.3.)

Parts C and C' of Figure 2.13 refer to a well in a densely fractured, highly permeable dike of infinite length and finite width in an otherwise confined, homogeneous, isotropic, consolidated aquifer of low hydraulic conductivity and high storage capacity. Characteristic of such a system are the two straight-line segments in a log-log plot of early and medium pumping times. The first segment has a slope of 0.5 and thus resembles that of the well in the single, vertical, plane fracture shown in Part B of Figure 2.13. At early time, the flow towards the well is exclusively through the dike, and this flow is parallel. At medium time, the adjacent aquifer starts yielding water to the dike. The dominant flow regime in the aquifer is then near-parallel to parallel, but oblique to the dike. In a log-log plot, this flow regime is reflected by a one-fourth slope straight-line segment. At late time, the dominant flow regime is pseudo-radial, which, in a semi-log plot, is reflected by a straight line.

The one-fourth slope straight-line segment does not always appear in a log-log plot; whether it does or not depends on the hydraulic diffusivity ratio between the dike and the adjacent aquifer. (We return to this subject in Section 19.3.)

2.9.2 Specific boundary conditions

When field data curves of drawdown versus time deviate from the theoretical curves of the main types of aquifer, the deviation is usually due to specific boundary conditions (e.g. partial penetration of the well, well-bore storage, recharge boundaries, or impermeable boundaries). Specific boundary conditions can occur individually (e.g. a partially penetrating well in an otherwise homogeneous, isotropic aquifer of infinite extent), but they often occur in combination (e.g. a partially penetrating well near a deeply incised river or canal). Obviously, specific boundary conditions can occur in all types of aquifers, but the examples we give below refer only to unconsolidated, confined aquifers.

Partial penetration of the well

Theoretical models usually assume that the pumped well fully penetrates the aquifer, so that the flow towards the well is horizontal. With a partially penetrating well, the condition of horizontal flow is not satisfied, at least not in the vicinity of the well. Vertical flow components are thus induced in the aquifer, and these are accompanied by extra head losses in and near the well. Figure 2.14 shows the effect of partial penetration. The extra head losses it induces are clearly reflected. (We return to this subject in Chapter 10.)

Well-bore storage

All theoretical models assume a line source or sink, which means that well-bore storage effects can be neglected. But all wells have a certain dimension and thus store some water, which must first be removed when pumping begins. The larger the diameter of the well, the more water it will store, and the less the condition of line source or

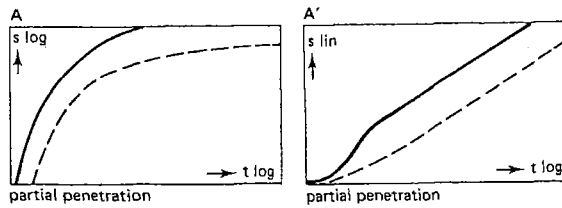


Figure 2.14 The effect of the well's partial penetration on the time-drawdown relationship in an unconsolidated, confined aquifer. The dashed curves are those of Parts A and A' of Figure 2.12

sink will be satisfied. Obviously, the effects of well-bore storage will appear at early pumping times, and may last from a few minutes to many minutes, depending on the storage capacity of the well. In a log-log plot of drawdown versus time, the effect of well-bore storage is reflected by a straight-line segment with a slope of unity. (We return to this subject in Section 15.1.1.)

If a pumping test is conducted in a large-diameter well and drawdown data from observation wells or piezometers are used in the analysis, it should not be forgotten that those data will also be affected by the well-bore storage in the pumped well. At early pumping time, the data will deviate from the theoretical curve, although, in a log-log plot, no early-time straight-line segment of slope unity will appear. Figure 2.15 shows the effect of well-bore storage on time-drawdown plots of observation wells or piezometers. (We return to this subject in Section 11.1.)

Recharge or impermeable boundaries

The theoretical curves of all the main aquifer types can also be affected by recharge or impermeable boundaries. This effect is shown in Figure 2.16. Parts A and A' of that figure show a situation where the cone of depression reaches a recharge boundary. When this happens, the drawdown in the well stabilizes. The field data curve then begins to deviate more and more from the theoretical curve, which is shown in the dashed segment of the curve. Impermeable (no-flow) boundaries have the opposite effect on the drawdown. If the cone of depression reaches such a boundary, the drawdown will double. The field data curve will then steepen, deviating upward from the theoretical curve. This is shown in Parts B and B' of Figure 2.16. (We return to this subject in Chapter 6.)

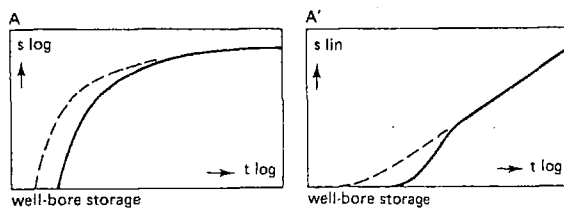


Figure 2.15 The effect of well-bore storage in the pumped well on the theoretical time-drawdown plots of observation wells or piezometers. The dashed curves are those of Parts A and A' of Figure 2.12

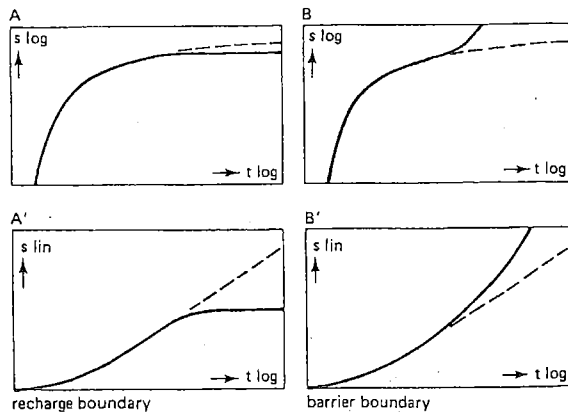


Figure 2.16 The effect of a recharge boundary (Parts A and A') and an impermeable boundary (Parts B and B') on the theoretical time-drawdown relationship in a confined unconsolidated aquifer. The dashed curves are those of Parts A and A' of Figure 2.12

2.10 Reporting and filing of data

2.10.1 Reporting

When the evaluation of the test data has been completed, a report should be written about the results. It is beyond the scope of this book to say what this report should contain, but it should at least include the following items:

- A map, showing the location of the test site, the well and the piezometers, and recharge and barrier boundaries, if any;
- A lithological cross-section of the test site, based on the data obtained from the bore holes, and showing the depth of the well screen and the number, depth, and distances of the piezometers;
- Tables of the field measurements made of the well discharge and the water levels in the well and the piezometers;
- Hydrographs, illustrating the corrections applied to the observed data, if applicable;
- Time-drawdown curves and distance-drawdown curves;
- The considerations that led to the selection of the theoretical model used for the analysis;
- The calculations in an abbreviated form, including the values obtained for the aquifer characteristics and a discussion of their accuracy;
- Recommendations for further investigations, if applicable;
- A summary of the main results.

2.10.2 Filing of data

A copy of the report should be kept on file for further reference and for use in any

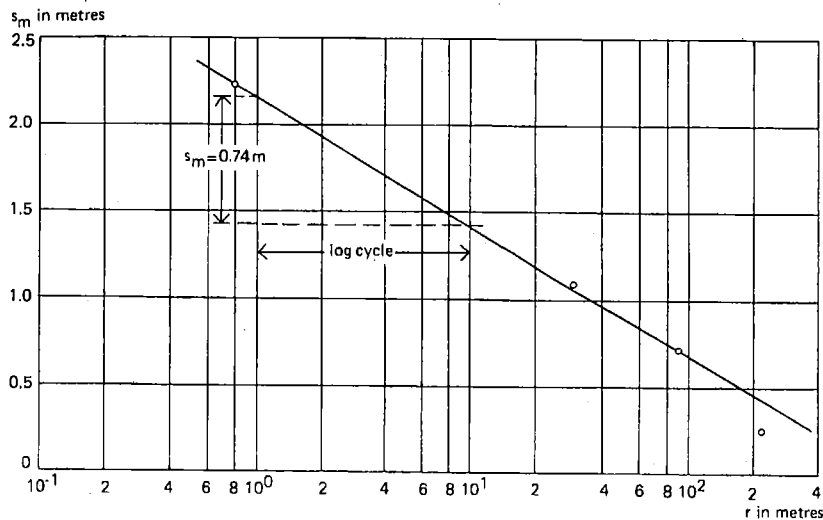


Figure 3.4 Analysis of data from pumping test 'Oude Korendijk' with the Thiem method, Procedure 3.2

This result agrees very well with the average value obtained with the Thiem method, Procedure 3.1.

Remarks

- Steady-state has been defined here as the situation where variations of the drawdown with time are negligible, or where the hydraulic gradient has become constant. The reader will know, however, that true steady state, i.e. drawdown variations are zero, is impossible in a confined aquifer;
- Field conditions may be such that considerable time is required to reach steady-state flow. Such long pumping times are not always required, however, because transient steady-state flow, i.e. flow under a constant hydraulic gradient, may be reached much earlier as we have shown in Example 3.1.

3.2 Unsteady-state flow

3.2.1 Theis's method

Theis (1935) was the first to develop a formula for unsteady-state flow that introduces the time factor and the storativity. He noted that when a well penetrating an extensive confined aquifer is pumped at a constant rate, the influence of the discharge extends outward with time. The rate of decline of head, multiplied by the storativity and summed over the area of influence, equals the discharge.

The unsteady-state (or Theis) equation, which was derived from the analogy between the flow of groundwater and the conduction of heat, is written as

$$s = \frac{Q}{4\pi KD} \int_u^{\infty} \frac{e^{-y}}{y} dy = \frac{Q}{4\pi KD} W(u) \quad (3.5)$$

where

s = the drawdown in m measured in a piezometer at a distance r in m from the well

Q = the constant well discharge in m^3/d

KD = the transmissivity of the aquifer in m^2/d

$u = \frac{r^2 S}{4KDt}$ and consequently $S = \frac{4KDtu}{r^2}$ (3.6)

S = the dimensionless storativity of the aquifer

t = the time in days since pumping started

$W(u) = -0.5772 - \ln u + u - \frac{u^2}{2.2!} + \frac{u^3}{3.3!} - \frac{u^4}{4.4!} + \dots$

The exponential integral is written symbolically as $W(u)$, which in this usage is generally read 'well function of u ' or 'Theis well function'. It is sometimes found under the symbol $-Ei(-u)$ (Jahnke and Embde 1945). A well function like $W(u)$ and its argument u are also indicated as 'dimensionless drawdown' and 'dimensionless time', respectively. The values for $W(u)$ as u varies are given in Annex 3.1.

From Equation 3.5, it will be seen that, if s can be measured for one or more values of r and for several values of t , and if the well discharge Q is known, S and KD can be determined. The presence of the two unknowns and the nature of the exponential integral make it impossible to effect an explicit solution.

Using Equations 3.5 and 3.6, Theis devised the 'curve-fitting method' (Jacob 1940) to determine S and KD . Equation 3.5 can also be written as

$$\log s = \log(Q/4\pi KD) + \log(W(u))$$

and Equation 3.6 as

$$\log(r^2/t) = \log(4KD/S) + \log(u)$$

Since $Q/4\pi KD$ and $4KD/S$ are constant, the relation between $\log s$ and $\log(r^2/t)$ must be similar to the relation between $\log W(u)$ and $\log(u)$. Theis's curve-fitting method is based on the fact that if s is plotted against r^2/t and $W(u)$ against u on the same log-log paper, the resulting curves (the data curve and the type curve, respectively) will be of the same shape, but will be horizontally and vertically offset by the constants $Q/4\pi KD$ and $4KD/S$. The two curves can be made to match. The coordinates of an arbitrary matching point are the related values of s , r^2/t , u , and $W(u)$, which can be used to calculate KD and S with Equations 3.5 and 3.6.

Instead of using a plot of $W(u)$ versus u (normal type curve) in combination with a data plot of s versus r^2/t , it is frequently more convenient to use a plot of $W(u)$ versus $1/u$ (reversed type curve) and a plot of s versus t/r^2 (Figure 3.5).

Theis's curve-fitting method is based on the assumptions listed at the beginning of this chapter and on the following limiting condition:

- The flow to the well is in unsteady state, i.e. the drawdown differences with time are not negligible, nor is the hydraulic gradient constant with time.

Procedure 3.3

- Prepare a type curve of the Theis well function on log-log paper by plotting values of $W(u)$ against the arguments $1/u$, using Annex 3.1 (Figure 3.5);
- Plot the observed data curve s versus t/r^2 on another sheet of log-log paper of the same scale;
- Superimpose the data curve on the type curve and, keeping the coordinate axes parallel, adjust until a position is found where most of the plotted points of the data curve fall on the type curve (Figure 3.6);
- Select an arbitrary match point A on the overlapping portion of the two sheets and read its coordinates $W(u)$, $1/u$, s , and t/r^2 . Note that it is not necessary for the match point to be located along the type curve. In fact, calculations are greatly simplified if the point is selected where the coordinates of the type curve are $W(u) = 1$ and $1/u = 10$;
- Substitute the values of $W(u)$, s , and Q into Equation 3.5 and solve for KD ;
- Calculate S by substituting the values of KD , t/r^2 , and u into Equation 3.6.

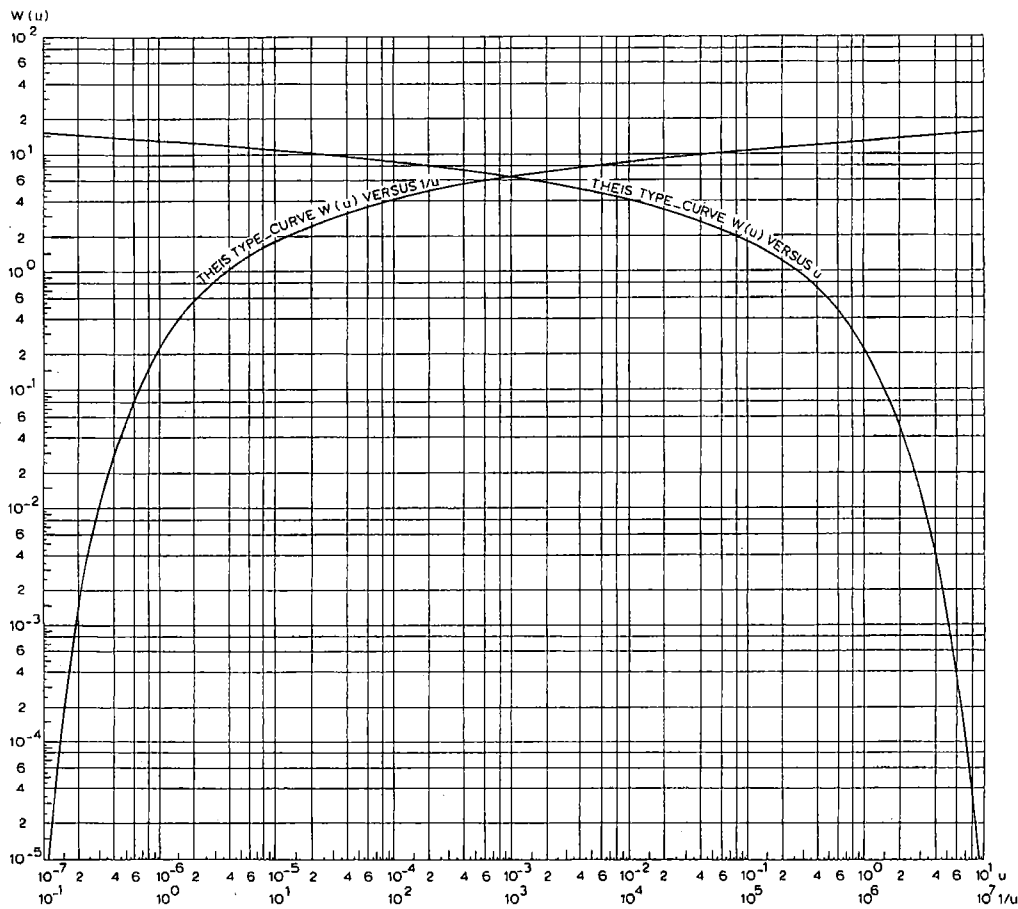


Figure 3.5 Theis type curve for $W(u)$ versus u and $W(u)$ versus $1/u$

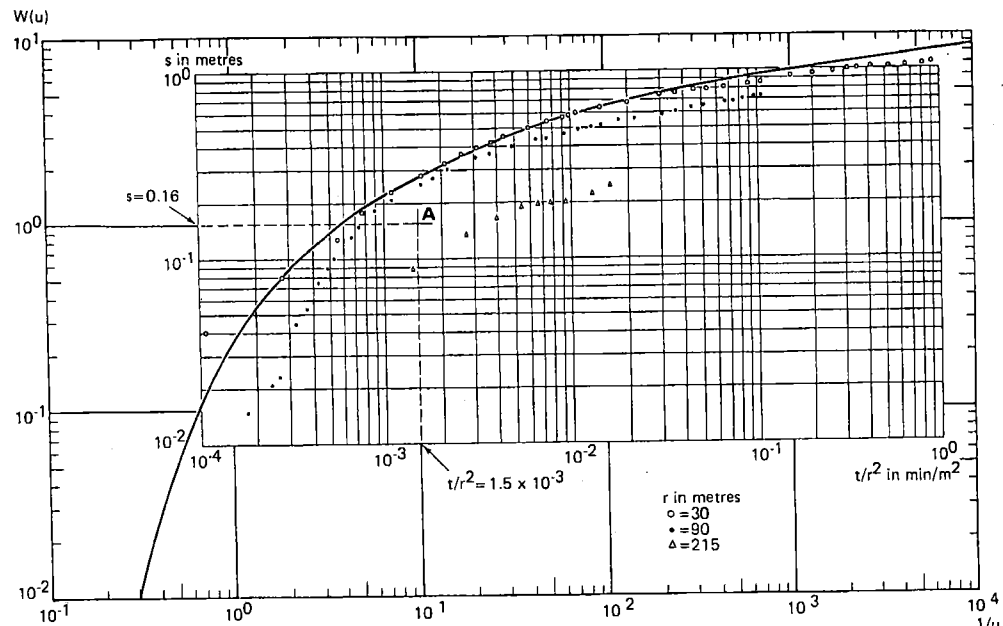


Figure 3.6 Analysis of data from pumping test 'Oude Korendijk' with the Theis method, Procedure 3.3

Remarks

- When the hydraulic characteristics have to be calculated separately for each piezometer, a plot of s versus t or s versus $1/t$ for each piezometer is used with a type curve $W(u)$ versus $1/u$ or $W(u)$ versus u , respectively;
- In applying the Theis curve-fitting method, and consequently all curve-fitting methods, one should, in general, give less weight to the early data because they may not closely represent the theoretical drawdown equation on which the type curve is based. Among other things, the theoretical equations are based on the assumptions that the well discharge remains constant and that the release of the water stored in the aquifer is immediate and directly proportional to the rate of decline of the pressure head. In fact, there may be a time lag between the pressure decline and the release of stored water, and initially also the well discharge may vary as the pump is adjusting itself to the changing head. This probably causes initial disagreement between theory and actual flow. As the time of pumping extends, these effects are minimized and closer agreement may be attained;
- If the observed data on the logarithmic plot exhibit a flat curvature, several apparently good matching positions, depending on personal judgement, may be obtained. In such cases, the graphical solution becomes practically indeterminate and one must resort to other methods.

Example 3.3

The Theis method will be applied to the unsteady-state data from the pumping test

'Oude Korendijk' listed in Table 3.1. Figure 3.6 shows a plot of the values of s versus t/r^2 for the piezometers H_{30} , H_{90} and H_{215} matched with the Theis type-curve, $W(u)$ versus $1/u$. The reader will note that for late pumping times the points do not fall exactly on the type curve. This may be due to leakage effects because the aquifer was not perfectly confined. Note the anomalous drawdown behaviour of piezometer H_{215} already noticed in Example 3.2. In the matching procedure, we have discarded the data of this piezometer. The match point A has been so chosen that the value of $W(u) = 1$ and the value of $1/u = 10$. On the sheet with the observed data, the match point A has the coordinates $s_A = 0.16$ m and $(t/r^2)_A = 1.5 \times 10^{-3} \text{ min/m}^2 = 1.5 \times 10^{-3}/1440 \text{ d/m}^2$. Introducing these values and the value of $Q = 788 \text{ m}^3/\text{d}$ into Equations 3.5 and 3.6 yields

$$KD = \frac{Q}{4\pi S_A} W(u) = \frac{788}{4 \times 3.14 \times 0.16} \times 1 = 392 \text{ m}^2/\text{d}$$

and

$$S = \frac{4KD(t/r^2)_A}{1/u} = 4 \times 392 \times \frac{1.5 \times 10^{-3}}{1440} \times \frac{1}{10} = 1.6 \times 10^{-4}$$

3.2.2 Jacob's method

The Jacob method (Cooper and Jacob 1946) is based on the Theis formula, Equation 3.5

$$s = \frac{Q}{4\pi KD} W(u) = \frac{Q}{4\pi KD} (-0.5772 - \ln u + u - \frac{u^2}{2.2!} + \frac{u^3}{3.3!} - \dots)$$

From $u = r^2S/4KDt$, it will be seen that u decreases as the time of pumping t increases and the distance from the well r decreases. Accordingly, for drawdown observations made in the near vicinity of the well after a sufficiently long pumping time, the terms beyond $\ln u$ in the series become so small that they can be neglected. So for small values of u ($u < 0.01$), the drawdown can be approximated by

$$s = \frac{Q}{4\pi KD} (-0.5772 - \ln \frac{r^2S}{4KDt})$$

with

an error less than	1%	2%	5%	10%
for u smaller than	0.03	0.05	0.1	0.15

After being rewritten and changed into decimal logarithms, this equation reduces to

$$s = \frac{2.30Q}{4\pi KD} \log \frac{2.25KDt}{r^2S} \quad (3.7)$$

Because Q , KD , and S are constant, if we use drawdown observations at a short distance r from the well, a plot of drawdown s versus the logarithm of t forms a straight line (Figure 3.7). If this line is extended until it intercepts the time-axis where $s = 0$, the interception point has the coordinates $s = 0$ and $t = t_0$. Substituting these values into Equation 3.7 gives

$$0 = \frac{2.30Q}{4\pi KD} \log \frac{2.25KDt_0}{r^2 S}$$

and because $\frac{2.30Q}{4\pi KD} \neq 0$, it follows that $\frac{2.25KDt_0}{r^2 S} = 1$

or

$$S = \frac{2.25KDt_0}{r^2} \quad (3.8)$$

The slope of the straight line (Figure 3.7), i.e. the drawdown difference Δs per log cycle of time $\log t/t_0 = 1$, is equal to $2.30Q/4\pi KD$. Hence

$$KD = \frac{2.30Q}{4\pi \Delta s} \quad (3.9)$$

Similarly, it can be shown that, for a fixed time t , a plot of s versus r on semi-log paper forms a straight line and the following equations can be derived

$$S = \frac{2.25KDt}{r_0^2} \quad (3.10)$$

and

$$KD = \frac{2.30Q}{2\pi \Delta s} \quad (3.11)$$

If all the drawdown data of all piezometers are used, the values of s versus t/r^2 can be plotted on semi-log paper. Subsequently, a straight line can be drawn through the

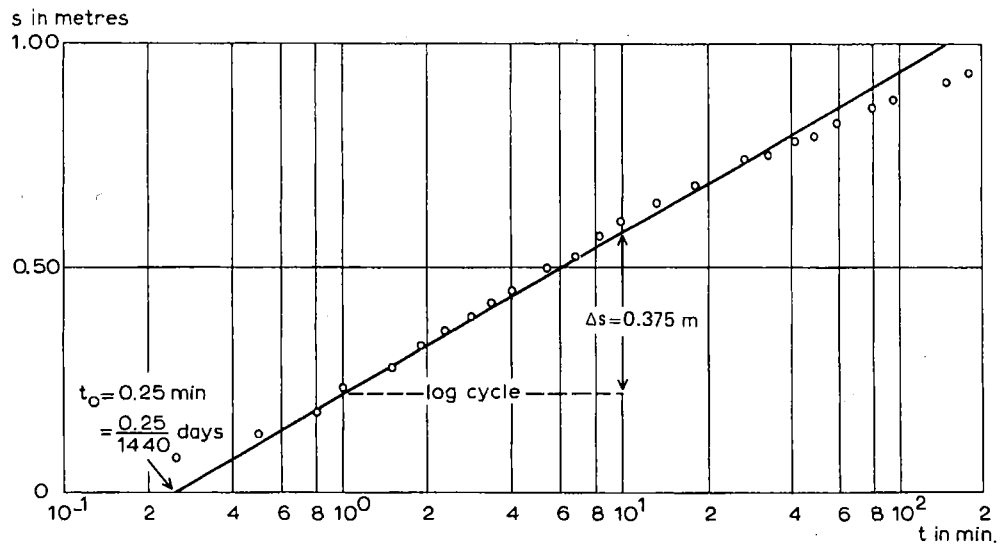


Figure 3.7 Analysis of data from pumping test 'Oude Korendijk' ($r = 30$ m) with the Jacob method, Procedure 3.4

plotted points. Continuing with the same line of reasoning as above, we derive the following formulas

$$S = 2.25KD(t/r^2)_0 \quad (3.12)$$

and

$$KD = \frac{2.30Q}{4\pi\Delta s} \quad (3.13)$$

Jacob's straight-line method can be applied in each of the three situations outlined above. (See Procedure 3.4 for $r = \text{constant}$, Procedure 3.5 for $t = \text{constant}$, and Procedure 3.6 when values of t/r^2 are used in the data plot.)

The following assumptions and conditions should be satisfied:

- The assumptions listed at the beginning of this chapter;
- The flow to the well is in unsteady state;
- The values of u are small ($u < 0.01$), i.e. r is small and t is sufficiently large.

The condition that u be small in confined aquifers is usually satisfied at moderate distances from the well within an hour or less. The condition $u < 0.01$ is rather rigid. For a five or even ten times higher value ($u < 0.05$ and $u < 0.10$), the error introduced in the result is less than 2 and 5%, respectively. Further, a visual inspection of the graph in the range $u < 0.01$ and $u < 0.1$ shows that it is difficult, if not impossible, to indicate precisely where the field data start to deviate from the straight-line relationship. For all practical purposes, therefore, we suggest using $u < 0.1$ as a condition for Jacob's method.

The reader will note that the use of Equation 3.7 for the determination of the difference in drawdown $s_1 - s_2$ between two piezometers at distances r_1 and r_2 from the well leads to an expression that is identical to the Thiem formula (Equation 3.2).

Procedure 3.4 (for r is constant)

- For one of the piezometers, plot the values of s versus the corresponding time t on semi-log paper (t on logarithmic scale), and draw a straight line through the plotted points (Figure 3.7);
- Extend the straight line until it intercepts the time axis where $s = 0$, and read the value of t_0 ;
- Determine the slope of the straight line, i.e. the drawdown difference Δs per log cycle of time;
- Substitute the values of Q and Δs into Equation 3.9 and solve for KD . With the known values of KD and t_0 , calculate S from Equation 3.8.

Remarks

- Procedure 3.4 should be repeated for other piezometers at moderate distances from the well. There should be a close agreement between the calculated KD values, as well as between those of S ;
- When the values of KD and S are determined, they are introduced into the equation $u = r^2S/4KDt$ to check whether $u < 0.1$, which is a practical condition for the applicability of the Jacob method.

Example 3.4

For this example, we use the drawdown data of the piezometer H_{30} in 'Oude Korendijk' (Table 3.1). We plot these data against the corresponding time data on semi-log paper (Figure 3.7), and fit a straight line through the plotted points. The slope of this straight line is measured on the vertical axis $\Delta s = 0.375$ m per log cycle of time. The intercept of the fitted straight line with the absciss (zero-drawdown axis) is $t_0 = 0.25$ min = 0.25/1440 d. The discharge rate $Q = 788$ m³/d. Substitution of these values into Equation 3.9 yields

$$KD = \frac{2.30Q}{4\pi\Delta s} = \frac{2.30 \times 788}{4 \times 3.14 \times 0.375} = 385 \text{ m}^2/\text{d}$$

and into Equation 3.8

$$S = \frac{2.25KDt_0}{r^2} = \frac{2.25 \times 385}{30^2} \times \frac{0.25}{1440} = 1.7 \times 10^{-4}$$

Substitution of the values of KD , S , and r into $u = r^2S/4KDt$ shows that, for $t > 0.001$ d or $t > 1.4$ min, $u < 0.1$, as is required. The departure of the time-drawdown curve from the theoretical straight line is probably due to leakage through one of the assumed 'impermeable' layers.

The same method applied to the data collected in the piezometer at 90 m gives: $KD = 450$ m²/d and $S = 1.7 \times 10^{-4}$ with $u < 0.1$ for $t > 11$ min. This result is less reliable because few points are available between $t = 11$ min. and the time that leakage probably starts to influence the drawdown data.

Procedure 3.5 (t is constant)

- Plot for a particular time t the values of s versus r on semi-log paper (r on logarithmic scale), and draw a straight line through the plotted points (Figure 3.8);
- Extend the straight line until it intercepts the r axis where $s = 0$, and read the value of r_0 ;
- Determine the slope of the straight line, i.e. the drawdown difference Δs per log cycle of r ;
- Substitute the values of Q and Δs into Equation 3.11 and solve for KD . With the known values of KD and r_0 , calculate S from Equation 3.10.

Remarks

- Note the difference in the denominator of Equations 3.9 and 3.11;
- The data of at least three piezometers are needed for reliable results;
- If the drawdown in the different piezometers is not measured at the same time, the drawdown at the chosen moment t has to be interpolated from the time-drawdown curve of each piezometer used in Procedure 3.4;
- Procedure 3.5 should be repeated for several values of t . The values of KD thus obtained should agree closely, and the same holds true for values of S .

Example 3.5

Here, we plot the (interpolated) drawdown data from the piezometers of 'Oude Korendijk' for $t = 140$ min ≈ 0.1 d against the distances between the piezometers and the well (Figure 3.8). In the previous examples, we explained why we discarded the point

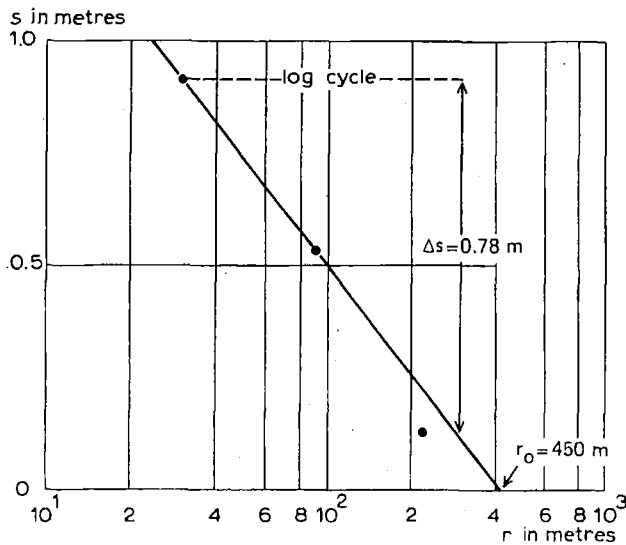


Figure 3.8 Analysis of data from pumping test 'Oude Korendijk' ($t = 140$ min) with the Jacob method, Procedure 3.5

of piezometer H_{215} . The slope of the straight line $\Delta s = 0.78$ m and the intercept with the absciss $r_0 = 450$ m. The discharge rate $Q = 788$ m³/d. Substitution of these values into Equation 3.11 yields

$$KD = \frac{2.30Q}{2\pi\Delta s} = \frac{2.30 \times 788}{2 \times 3.14 \times 0.78} = 370 \text{ m}^2/\text{d}$$

and into Equation 3.10

$$S = \frac{2.25KDt}{r_0^2} = \frac{2.25 \times 370 \times 0.1}{450^2} = 4.1 \times 10^{-4}$$

Procedure 3.6 (based on s versus t/r^2 data plot)

- Plot the values of s versus t/r^2 on semi-log paper (t/r^2 on the logarithmic axis), and draw a straight line through the plotted points (Figure 3.9);
- Extend the straight line until it intercepts the t/r^2 axis where $s = 0$, and read the value of $(t/r^2)_0$;
- Determine the slope of the straight line, i.e. the drawdown difference Δs per log cycle of t/r^2 ;
- Substitute the values of Q and Δs into Equation 3.13 and solve for KD . Knowing the values of KD and $(t/r^2)_0$, calculate S from Equation 3.12.

Example 3.6

As an example of the Jacob method, Procedure 3.6, we use the values of t/r^2 for all the piezometers of 'Oude Korendijk' (Table 3.1). In Figure 3.9, the values of s are plotted on semi-log paper against the corresponding values of t/r^2 . Through those points, and neglecting the points for H_{215} , we draw a straight line, which intercepts

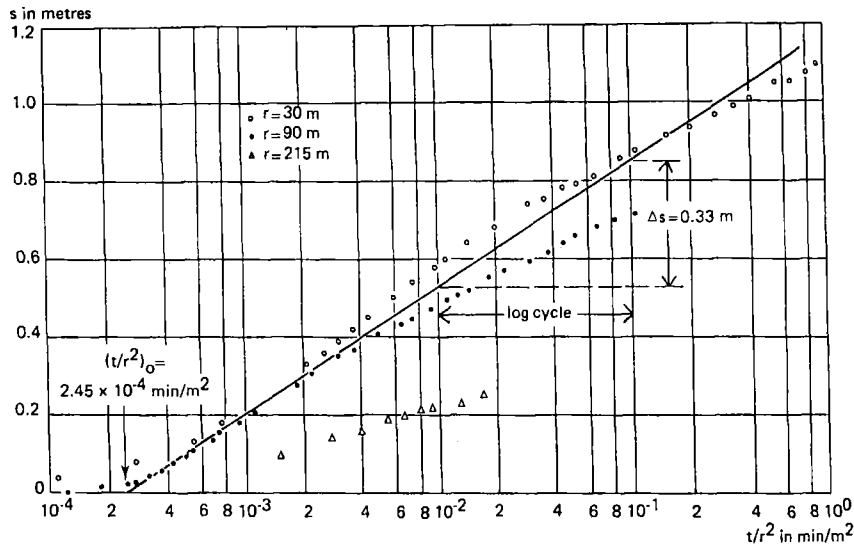


Figure 3.9 Analysis of data from pumping test 'Oude Korendijk' with the Jacob method, Procedure 3.6

the $s = 0$ axis (absciss) in $(t/r^2)_0 = 2.45 \times 10^{-4} \text{ min/m}^2$ or $(2.45/1440) \times 10^{-4} \text{ d/m}^2$. On the vertical axis, we measure the drawdown difference per log cycle of t/r^2 as $\Delta s = 0.33 \text{ m}$. The discharge rate $Q = 788 \text{ m}^3/\text{d}$. Introducing these values into Equation 3.13 gives

$$KD = \frac{2.30Q}{4\pi\Delta s} = \frac{2.30 \times 788}{4 \times 3.14 \times 0.33} = 437 \text{ m}^2/\text{d}$$

and into Equation 3.12

$$S = 2.25KD(t/r^2)_0 = 2.25 \times 437 \times \frac{2.45}{1440} \times 10^{-4} = 1.7 \times 10^{-4}$$

3.3 Summary

Using data from the pumping test 'Oude Korendijk' (Figure 3.2 and Table 3.1), we have illustrated the methods of analyzing (transient) steady and unsteady flow to a well in a confined aquifer. Table 3.3 summarizes the values we obtained for the aquifer's hydraulic characteristics.

When we compare the results of Table 3.3, we can conclude that the values of KD and S agree very well, except for those of the last two methods. The differences in the results are due to the fact that the late-time data have probably been influenced by leakage and that graphical methods of analysis are never accurate. Minor shifts of the data plot are often possible, giving an equally good match with a type curve, but yielding different values for the aquifer characteristics. The same is true for a semi-log plot whose points do not always fit on a straight line because of measuring

errors or otherwise. The analysis of the Jacob 2 method, for example, is weak, because the straight line has been fitted through only two points, the third point, that of the piezometer H₂₁₅, being unreliable. The anomalous behaviour of this far-field piezometer may be due to leakage effects, heterogeneity of the aquifer (the transmissivity at H₂₁₅ being slightly higher than closer to the well), or faulty construction (partly clogged).

We could thus conclude that the aquifer at 'Oude Korendijk' has the following parameters: $KD = 390 \text{ m}^2/\text{d}$ and $S = 1.7 \times 10^{-4}$.

Table 3.3 Hydraulic characteristics of the confined aquifer at 'Oude Korendijk', obtained by the different methods

Method	KD (m ² /d)	S (-)
Thiem 1	385	-
Thiem 2	390	-
Theis	392	1.6×10^{-4}
Jacob 1	385	1.7×10^{-4}
Jacob 2	370	4.1×10^{-4}
Jacob 3	437	1.7×10^{-4}